AUTHOR(S)	Mattila Heta, Khorobrykh Sergey, Tyystjärvi Esa
TITLE	Both external and internal factors induce heterogeneity in senescing leaves of deciduous trees
YEAR	2024
DOI	10.1071/FP24012
CITATION	Mattila Heta, Khorobrykh Sergey, Tyystjärvi Esa (2024) Both external and internal factors induce heterogeneity in senescing leaves of deciduous trees. Functional Plant Biology 51, FP24012. https://doi.org/10.1071/FP24012

Cite this: Mattila H et al. (2024) Both external and internal factors induce heterogeneity in senescing leaves of deciduous trees. Functional Plant Biology 51, FP24012. doi:10.1071/FP24012

Both external and internal factors induce heterogeneity in senescing leaves of deciduous trees

Heta Mattila[1,2]*, Sergey Khorobrykh[1], Esa Tyystjärvi[1]

[1]Molecular Plant Biology, University of Turku, Finland

[2]Centre for Environmental and Marine Studies, University of Aveiro, Portugal

*Corresponding author email: h.mattila@ua.pt

Abstract

Autumn senescence is characterized by spatial and temporal heterogeneity. We show that senescing birch leaves possessed lower PSII activity (probed by the F_V/F_M chlorophyll *a* fluorescence parameter) during late than during early autumn. We confirmed that PSII repair slows down with decreasing temperature, while rates of photodamage and recovery, measured under laboratory conditions at 20°C, were similar in these leaves. We propose that low temperatures during late autumn hinder repair and lead to accumulation of non-functional PSII units in senescing leaves. Next, fluorescence imaging of birch revealed that chlorophyll preferentially disappeared from inter-veinal leaf areas. These areas showed no recovery capacity and low non-photochemical quenching while green veinal areas of senescing leaves resembled green leaves. However, green and yellow leaf areas showed similar values of photochemical quenching. Analyses of thylakoids isolated from maple leaves revealed that red leaves contained high amounts of carotenoids and α-tocopherol, and our calculations suggest that α-tocopherol was synthesized during autumn. Thylakoids isolated from red maple leaves produced little singlet oxygen, probably due to the high antioxidant content. However, the rate of PSII photodamage did not decrease. The data show that the heterogeneity of senescing leaves must be taken into account to fully understand autumn senescence.

Keywords: *Acer platanoides*; Anthocyanin; Autumnal; *Betula pendula*; *Betula pubescens*; Photoinhibition; Reactive oxygen species; SOSG

Summary text: Often, autumn senescence does not proceed uniformly, as green pigments (chlorophylls) disappear and red pigments (anthocyanins) appear unevenly along leaf blades of senescing leaves of deciduous trees. We show that only green parts of senescing leaves show efficient recovery from photodamage and that red parts contain high amounts of antioxidants and thus, produce little harmful reactive oxygen species (singlet oxygen). To fully understand tree physiology, the heterogenous nature of (autumn) senescence should be considered.

Introduction

During (autumn) senescence, plants degrade chlorophylls, proteins (including the complexes of the photosynthetic electron transport chain) and other macromolecules. While senescence is a regulated process (for reviews, see Kuai *et al*. 2018; Sasi *et al*. 2022), it is also an inhomogeneous process, as chlorophyll degradation and other senescence-related phenomena do not often proceed uniformly, neither in all leaves of a tree (Mattila *et al*. 2018; Kitao *et al*. 2022) nor within a single leaf (Dodge 1970; Keskitalo *et al*. 2005; Ruberti *et al*. 2014; Junker and Ensminger 2016). In silver birch (*Betula pendula*), for example, cells close to veins typically retain chlorophyll longer than cells in other leaf areas (Quirino *et al*. 2000; Mattila *et al*. 2021). A similar pattern was observed in senescing tobacco (*Nicotiana tabacum*) leaves where the inter-veinal areas containing low amounts of chlorophyll also showed low PSII activity and low expression of many photosynthesis genes (Niewiadomska *et al*. 2009). However, some senescence-associated genes were upregulated (in comparison to non-senescing leaves) even in the green veinal areas of senescing leaves (Niewiadomska *et al*. 2009).

Senescing leaves of many species synthesize anthocyanins, which may protect the leaves from excess light or from insect herbivory (Renner and Zohner 2019; Agati *et al*. 2021; Hughes *et al*. 2022; Lev-Yadun 2022) or provide a sink for carbon skeletons produced at the last phase of senescence (Mattila and Tyystjärvi 2023). Anthocyanins typically accumulate heterogeneously, too, both between and within leaves (Anderson and Ryser 2015; Kitao *et al*. 2022; Mattila and Tyystjärvi 2023). Some of the variation may originate from different light environments of leaves (García-Plazaola *et al*. 2003; Anderson and Ryser 2015; Kitao *et al*. 2022). In addition, differences in the translocation capacity of nutrients or photosynthates may explain the variability (Lihavainen *et al*. 2021; Mattila and Tyystjärvi 2023).

It has been suggested that the degradation of photosynthetic complexes promotes production of reactive oxygen species in the chloroplasts of senescing leaves (Cheeseman 2009; Shi *et al*. 2012; Krieger-Liszkay *et al*. 2019; Mattila *et al*. 2021). In addition, senescing leaves, as well as other leaves with low chlorophyll content, experience faster photoinhibition (light-induced irreversible damage to Photosystem II (PSII); see Tyystjärvi 2013) than greener leaves (Pätsikkä *et al*. 2002; Mattila *et al*. 2021; Serôdio and Campbell 2021). Nevertheless, photosynthesis functions remarkably well in senescing leaves until almost all chlorophyll has been degraded, using the remaining complexes of the electron transport machinery (Keskitalo *et al*. 2005; Rantala *et al*. 2023). For a comparison, prematurely bleached summer leaves of a maple (*Acer saccharinum*) exhibit much lower PSII activities (Uzarević *et al*. 2011) than normally senescing leaves with a similar, low chlorophyll content (Moy *et al*. 2015).

Here, spatial and temporal heterogeneity of autumnal senescence was studied in leaves of deciduous trees. First, we investigated if the advancement of autumn affects photoinhibition or repair in senescing birch leaves. Then, chlorophyll *a* fluorescence imaging was used to further study these processes in differently coloured (green and yellow) areas of senescing leaves. In addition, to compare yellow and red (anthocyanic) leaf areas, also maple leaves were used. Finally, thylakoids were isolated from green, yellow and red maple leaves, to study photoinhibition in optically similar samples and to measure pigment compositions as well as production of reactive oxygen species. We show that both environmental factors (temperature) and internal factors (protective pigments) affect senescing leaves' capacities to protect themselves from high light.

Materials and methods

Plant material

Silver birch or downy birch (*B. pendula* Roth. and *Betula pubescens* Ehrh., respectively) and Norway maple (*Acer platanoides* L.) leaves were collected on 26/5/2020–21/10/2020, 15/7/2021, 24/9/2021–9/10/2021, 3/10/2022–3/11/2022 and 20–27/9/2023 from the height of 1–2 m, from trees growing in small city parks (Turku, Finland). Measurements and treatments on the leaves were then conducted in laboratory conditions on the collection day, unless otherwise mentioned.

Thylakoid membranes were isolated from dark-acclimated (≥ 30 min) maple leaves as follows; main veins were removed and the rest of the leaf material was ground in a blender for about 10 s (at 4 °C), after which the isolation was further conducted as described by Hakala *et al*. (2005). Thylakoids were stored at -75 °C in storage buffer consisting of 10 mM 4-(2-hydroxyethyl)-1-piperazineethanesulfonic acid (HEPES; pH 7.4), 0.5 M sorbitol, 10 mM $MgCl_2$, and 5 mM NaCl.

Measurements of chlorophylls, carotenoids and α-tocopherol

Leaf chlorophyll contents were measured with an optical SPAD method (MultispeQ v1, PhotosynQ Inc., USA; see Hunt and Daughtry 2014). To calibrate the optical measurements, chlorophylls *a* and *b* were extracted in dimethylformamide (DMF) in darkness at 4 °C for 4–10 days, until the leaf disc (d = 6 mm) was completely bleached. After the extraction, chlorophylls were quantified spectrophotometrically (Porra *et al*. 1989) and the results were compared with the optical SPAD measurements from the same leaves.

Chlorophyll values measured with MultispeQ showed a curvilinear response to chlorophyll content measured with extraction in DMF (Fig. S1). The response also slightly differed between birch and maple (Fig. S1). To convert the optical SPAD values to µg chlorophylls *a* and *b* cm^{-2}, the following polynomial equations (intercept = 0) were obtained after fitting the data points in Microsoft excel (Fig. S1):

Chlorophyll *a* + *b* content in birch leaves, µg cm^{-2} = MultispeQ $value^2$ x 0.0343 - MultispeQ value x 0.1507

Chlorophyll *a* + *b* content in maple leaves, µg cm^{-2} = MultispeQ $value^2$ x 0.0226 + MultispeQ value x 0.0345

Chlorophylls *a* and *b* and total carotenoid contents of thylakoid suspensions were measured after extraction (≥ 10 min) in 80 % acetone (buffered with HEPES to pH 7.4) according to Porra *et al*. (1989) and Wellburn (1994), respectively. In addition, chlorophylls, different carotenoid species and α-tocopherol were measured from thylakoids, dissolved in methanol, with a 1100 series high performance liquid chromatography (HPLC) system (Agilent Technologies, Palo Alto, CA), as described in Lehtimäki *et al*. (2011). Chlorophylls and carotenoids were identified by their spectra and quantified according to the peak area. Chlorophyll quantification was verified by the above-described spectroscopy method (Porra *et al*. 1989). α-tocopherol was identified and quantified with a standard (α-tocopherol, ≥ 96%; Sigma-Aldrich).

Illumination treatments

Leaves were illuminated with a sunlight simulator (SLHolland) with the photosynthetic photon flux density (PPFD) of 1300–2000 µmol $m^{-2}s^{-1}$ for one to four hours, as indicated. During the illumination, leaves were kept on a wet paper placed on a temperature-controlled metal block (set to 20 °C). After the illumination, leaves were let to recover for 4–14 h, as indicated, at room temperature or on a temperature-controlled metal block (set to 5 or 12 °C) under low light (PPFD

10–20 µmol m^{-2} s^{-1}) on a wet paper. Before and after the illumination, and after the recovery, leaves were dark-acclimated at room temperature, after which chlorophyll *a* fluorescence was measured (see below).

Thylakoids (50 µg chlorophyll ml^{-1}) were suspended in 27 µl (3 mm light path; in the case of singlet oxygen measurements; see below) or in 100 µl (1 cm light path; in the case of photoinhibition measurements; see below) of the storage buffer and illuminated (PPFD 2000 µmol m^{-2} s^{-1}) for 10–30 min, as indicated, at 20 °C. For photoinhibition experiments, thylakoids were illuminated with the sunlight simulator and for singlet oxygen measurements, with red light (obtained with a 650 nm long pass filter LL650; Corion, USA). In both the cases, thylakoid suspensions were regularly mixed during the illumination.

Chlorophyll *a* fluorescence

$(F_M-F_O)/F_M = F_V/F_M$ was measured with FluorPen (Photon System Instruments, Czech Republic) or with Open FluorCam FC 800-O/2504 (Photon Systems Instrument), after at least 30 min (leaves) or 5 min (thylakoids) in the dark. $(F_M'-F_O')/F_M' = F_V'/F_M'$ was measured with MultispeQ (PhotosynQ) under darkness, after 30 min in the dark.

Fluorescence imaging was performed with Open FluorCam FC 800-O/2504 (Photon Systems Instrument), as follows. Always before the imaging, leaves were kept in darkness for at least 30 min. The measurement protocol started with a measurement of the F_O fluorescence level (only the low-intensity measuring flashes on; flash duration: 10 µs) after which a saturating flash (800 ms; photosynthetic photon flux density (PPFD) > 2500 µmol m^{-2} s^{-1}) was fired to measure F_M, to calculate F_V/F_M. Then red actinic light was switched on (PPFD ~265 or ~235 µmol m^{-2} s^{-1} for birch and maple leaves, respectively). Seven saturating flashes were fired during the actinic illumination and three more after the actinic light was switched off, to follow photochemical quenching $qL= (F_M'-F)/(F_M' - F_O')\times(F_O'/F)$ where $F_O' = 1/(1/F_O - 1/F_M + 1/F_M')$, according to Oxborough and Baker (1997) and Kramer *et al*. (2004) and non-photochemical quenching $NPQ = (F_M-F_M')/F_M'$.

For quantitative analyses of the fluorescence images, background (including holes and leaf areas containing no chlorophyll) was first manually excluded. In the case of senescing birch leaves, two separate leaf areas (areas close to the main veins and areas between the veins; Fig. S2) were defined. In the case of senescing maple leaves, up to nine circular areas (d = ~1 cm) were manually selected from each leaf and annotated as green, yellow or red, based on visual estimation. Careful visual inspection was done to target the same areas for analysis (as each leaf was imaged three

154 times; before and after the light treatment and after recovery). Fluorescence yields and parameter
155 values were averaged over the defined areas.

156 In the case of thylakoids, photoinhibition was quantified by calculating its rate constant in
157 SigmaPlot (SYSTAT) by fitting the decrease in the F_V/F_M parameter value to the first-order reaction
158 equation. The final rate constant of photoinhibition (k_{PI}) was achieved by calculating the rate
159 constants of PSII inactivation separately in the light (k_{LIGHT}) and in the dark (k_{DARK}) and by
160 subtracting the values of k_{DARK} from the values of k_{LIGHT}.

161 **Oxygen evolution**

162 The maximum rates of oxygen evolution of PSII were measured from thylakoid suspensions (10 µg
163 chlorophyll ml^{-1}) at 20 °C with an oxygen electrode (Hansatech; UK) in saturating white light
164 (PPFD > 2000 µmol m^{-2} s^{-1}) in the presence of an electron acceptor (0.5 mM 2,6-
165 dimethylbenzoquinone), otherwise as described by Hakala *et al*. (2005).

166 **Measurements of singlet oxygen**

167 Thylakoid suspensions were diluted with the storage buffer (50 µg chlorophyll ml^{-1}) and illuminated
168 at 20 °C for 10 min with red light (PPFD 2000 µmol m^{-2} s^{-1}) in the presence of 5 µM Singlet oxygen
169 sensor green (SOSG; Invitrogen). Before and after the illumination, SOSG fluorescence, excited
170 with 500 nm light (full width at half maximum 10 nm), was measured with a QEPro spectrometer
171 (Ocean Insights). Quantification was done by integrating the signal at 529–532 nm, and subtracting
172 the signal obtained before the illumination.

173 **Weather data**

174 Weather data were obtained from the Finnish Meteorological Institute.

175 **Statistical tests and figures**

176 Leaves ($n \geq 3$) were collected from three or four individual trees, except for Fig. 1c–e, in which
177 case they were collected from a single tree. Three separate isolations of thylakoids were conducted,
178 each one with leaves collected from a different tree, except in the case of α-tocopherol analysis, in
179 which case only two isolations (4 replicates) were used. In the case of spring thylakoids, only one
180 isolation (4 replicates) was done. T-tests (heteroscedastic) were calculated in Microsoft Excel.
181 Statistically significant differences are indicated in the respective figures with asterisks; $P \leq 0.05$ =
182 *, $P \leq 0.01$ = ** and $P \leq 0.001$ = ***. Figures were prepared with SigmaPlot (SYSTAT).

183 **Results**

184 **F_V/F_M values were low in senescing birch leaves during late autumn**

185 Birch leaves were collected from outdoors-grown trees during spring, summer and autumn and their
186 PSII activities were probed by the F_V/F_M fluorescence parameter, measured after 30 min dark-
187 acclimation. In general, the F_V/F_M values stayed high (> 0.7) even in leaves with low chlorophyll
188 content (i.e. in young and senescing leaves), however, leaves collected during late autumn showed
189 low (< 0.6) F_V/F_M values (Fig. 1a).

190 To see if the F_V/F_M values were low during late autumn because senescing leaves become more
191 vulnerable to the damaging reaction of PSII photoinhibition or because their capacity to repair PSII
192 decreases towards the end of autumn, green and senescing leaves were collected from a single
193 senescing birch tree at four different dates during autumn. The dates were chosen so that the leaves
194 were collected when the tree was mainly green and just started to senesce, at the middle of
195 senescence (before and after a cold period) and when the tree had dropped almost all of its leaves
196 (Figs. 1b and S3). Senescing leaves were selected so that all leaves within one type of sample had,
197 on the average, a similar chlorophyll content (Fig. 1c) and thus, were at the same phase of
198 senescence. The average chlorophyll content of the green leaves decreased when autumn progressed
199 (Fig. 1c), presumably because the number of leaves that had not yet started to senesce was
200 decreasing. The observation that senescing leaves showed lower F_V/F_M values when they were
201 collected later during the autumn (even though having the same chlorophyll contents) was
202 confirmed (Fig. 1a,d).

203 Leaves were then given a high light treatment after which they were let to recover few hours under
204 low light, at room temperature (20 °C). Unsurprisingly, green leaves were photoinhibited to a lesser
205 degree than senescing leaves and also recovered better (almost to 100 % of control values; Fig. 1e).
206 When all individual photoinhibition measurements were plotted against the chlorophyll contents of
207 the leaves, it could be seen that the high-light-induced decline in the F_V/F_M values increased
208 curvilinearly with decreasing chlorophyll content of the leaf (Fig. S4). However, the collection date
209 had no effect on the extent of photoinhibition or on the subsequent recovery in low light in
210 senescing leaves (Fig. 1e). In the green leaves collected at the last date, recovery was slightly
211 slower, compared to other green leaves, but this was likely due to the low chlorophyll content of
212 this group (Fig. 1c,e).

213 Senescing leaves collected after a cold period showed the lowest F_V/F_M values (prior the high light
214 treatment) (Fig. 1b,d). Therefore, the effect of temperature on the recovery was tested. For this,
215 leaves were illuminated at 20 °C, as previously, but then let to recover at 5, 12 or 20 °C (Fig. 1f–h).

The amount of recovery obtained decreased with decreasing temperature (Fig. 1g). Still, even at 5 °C, green and senescing leaves could repair 50 % and 30 % of the damage, respectively (Fig. 1h). The temperature response of recovery was similar in green and senescing leaves (Fig. 1h).

In birch, leaf areas close to veins senesced last

The experiments described above showed F_V/F_M values measured with a conventional fluorometer, which averages the signal over a certain leaf area. However, senescing birch leaves do not turn uniformly from green to yellow, but areas close to main veins typically stay green longer than other areas (Fig. 2a). To take the heterogeneous nature of senescence into account, fluorescence imaging was performed (Fig. 2b–m). In addition, after an initial F_V/F_M measurement, an actinic light of moderate intensity (PPFD ~265 μmol m^{-2} s^{-1}) was switched on for several minutes to record NPQ (non-photochemical quenching) and qL (photochemical quenching) (Fig. S5). Green leaves produced relatively even fluorescence images and heterogeneity in the fluorescence signal was not systematically related to a particular position within the leaf (Fig. 2b–c; for quantification, see Fig. 2n). In senescing leaves, on the contrary, the greenest areas close to main veins emitted more fluorescence than the yellower areas between veins (Fig. 2d–e,n). Similarly as above (Fig. 1), F_V/F_M values, when averaged over a whole senescing leaf, were lower (0.67) in senescing leaves than in green leaves (0.79). However, F_V/F_M values in the green areas of senescing leaves (0.73) were fairly close to the values of green leaves. On the other hand, F_V/F_M values in the yellow areas of senescing leaves were low (0.60).

Next, leaves were given a high-light treatment, after which the fluorescence imaging was repeated. Clear decreases in the F_M and F_V/F_M values were observed in both green and senescing leaves (Fig. 2f–i). Again, the high-light-induced decline of the F_V/F_M parameter value was smaller in green leaves (to 72 % of the control value) than in senescing leaves (to 52 % of the control value; Fig. 2n). F_V/F_M values of the green parts of yellow leaves decreased less (to 59 % of the control value) than those of the yellow parts (to 42 % of the control; Fig. 2n). Here, the difference between green and senescing leaves was bigger than in Fig. 1, presumably due to the lower chlorophyll content of the senescing leaves used in Fig. 2 (according to a visual estimation).

After the leaves were let to recover, F_V/F_M values of green leaves returned to 90 % of the initial values (Fig. 2j–k,n). Senescing leaves recovered heterogeneously; while F_V/F_M values in the green areas near veins recovered to 75 % of the initial values, F_V/F_M values in the yellow areas between veins recovered only marginally (Fig. 2l–m,n). Accordingly, fluorescence seemed to diminish especially from leaf areas between veins, most clearly seen in the images of the F_M values (Fig. 2l–

m). On the contrary, unequal recovery was seen in green leaves only in the areas close to the edges which were often visually damaged already before the illumination (Fig. 2a,j–k).

In general, senescing leaves induced less NPQ (during the actinic illumination) than green leaves, and the difference was more pronounced in the yellow areas between veins than in the green vein areas (Fig. 2n). After the high light treatment, less NPQ was induced (except in green leaves when measured after 1.1 min of illumination with the actinic light). After the recovery, NPQ measured after 1.1 min and 3.6 min of the actinic illumination behaved differently; the early NPQ induction further diminished whereas NPQ at the later time point again increased (Fig. 2n). Photochemical quenching increased after the high light treatment and decreased after the recovery, with no apparent differences between green and senescing leaves (Fig. 2n).

Green sections of senescing maple leaves behaved very similarly as fully green leaves

Chlorophyll degradation is not the only visually observable heterogenous process in autumn senescence; also red pigments may accumulate unevenly in senescing leaves. Thus, fluorescence imaging was next performed on green and senescing maple leaves, the latter ones containing green, red and yellow sections (Figs. 3a–b and S6). Before the high light treatment, F_V/F_M values of green sections of senescing leaves were only slightly lower (0.75) than those of fully green leaves (0.76) while F_V/F_M values of yellow and red sections of senescing leaves were 0.67 and 0.64, respectively (Fig. 3c–n, for quantification, see Fig. 3o).

Similarly as in birch leaves, the high-light-induced decrease in F_V/F_M values was much stronger in those parts of senescing maple leaves that had a low chlorophyll content (i.e. red and yellow parts) than in green parts or in fully green maple leaves (Fig. 3o). Furthermore, F_V/F_M values of green leaves and green sections of senescing leaves recovered completely from the high light treatment during the recovery period (Fig. 3o), whereas F_V/F_M values of the yellow and red sections of senescing leaves recovered much less (Fig. 3o). In general, only small differences were observed between red and yellow sections of senescing maple leaves (Figs. 3).

NPQ and qL behaved quite similarly in maple as in birch; the high light treatment caused a decrease in NPQ induction under the moderate actinic light, and this decrease in NPQ capacity recovered only at the later measurement point (after 3.6 min of actinic illumination). Also qL increased and decreased due to the high light treatment and recovery, respectively (Fig. 3o). Like in birch, NPQ was low in senescing maple leaves while qL was not much affected (Fig. 3o). NPQ and qL behaved similarly in red and yellow sections of senescing maple leaves.

Red senescing maple leaves contained more α-tocopherol and carotenoids than yellow or green leaves

To further study the possible differences of red and yellow senescing maple leaves, thylakoids were isolated from fully green maple leaves, and from red and yellow senescing leaves (see Table 1). All thylakoids were functional, as indicated by reasonable rates of PSII oxygen evolution, measured on chlorophyll basis (Fig. S7). Thylakoids isolated from senescing leaves, especially those isolated from red leaves, contained more α-tocopherol and carotenoids (normalized to chlorophyll content) than thylakoids isolated from green leaves (Fig. 4a–b). Most of the carotenoid species that increased in senescing leaves could not be identified (Fig. 4c; Table S1); of the recognized carotenoids, the xanthophyll cycle pigments (violaxanthin, antheraxanthin and zeaxanthin) as well as lutein and neoxanthin increased significantly only in thylakoids isolated from red senescing leaves (Fig. 4d). Zeaxanthin was not abundant in any of the thylakoids, which is expected as the leaves were kept in darkness before the thylakoid isolation.

To test the effects of the different amounts of tocopherols and carotenoids on photoinhibition, thylakoids were illuminated with high light. Thylakoids isolated from red senescing leaves produced the least singlet oxygen of all the thylakoids, and thylakoids isolated from green leaves the most (Fig. 4e). Next, PSII activity was estimated with the F_V/F_M parameter (measured after a short dark-acclimation; Fig. 4f) and photoinhibition was quantified by fitting the light-induced decline in the F_V/F_M values to a first-order reaction equation. The differences in the rate constants were not very big but, in any case,, thylakoids isolated from yellow senescing leaves exhibited slower photoinhibition, when dark-inactivation was taken into account, than thylakoids isolated from green or red leaves (Table 1). In all measurements, thylakoids isolated from green summer leaves resembled those of autumn green leaves but because the results from summer leaves are based on only one thylakoid isolation, no further analyses were performed.

Discussion

Usually, (autumn) senescence is not a homogenous process. Chlorophyll degradation may not begin at the same time in all leaves of a plant (Mattila *et al*. 2018) and different leaves often show different colours (Anderson and Ryser 2015; Mattila and Tyystjärvi 2023). Furthermore, senescence can proceed in a non-uniform manner also within a single leaf (Keskitalo *et al*. 2005; Niewiadomska *et al*. 2009). The heterogenous nature of senescence has received surprisingly little attention. Thus, we utilized fluorescence imaging, as well as other means, to investigate the reasons

and consequences for temporal and spatial heterogeneity in naturally senescing birch and maple leaves.

Fluorescence imaging reveals the heterogeneity of senescence

Some of the processes studied here, like the repair of PSII damage and induction of NPQ, differed between senescing and non-senescing leaves, as well as between green and yellow (or red) parts of a senescing leaf. Other parameters, like photochemical quenching, varied less (Figs. 2–3). These findings are in line with those of Niewiadomska *et al*. (2009) who observed that some senescence-associated genes were upregulated (when compared to non-senescing leaves) in all parts of a senescing leaf while expression of other genes greatly differed between green and yellow areas of senescing leaves. Thus, senescence may be initiated over the whole leaf but proceeds at different rates in different parts of the leaf.

The observed high photochemical quenching in senescing leaves likely reflects the need to keep photosynthesis going on, in order to produce energy for nutrient resorption. In birch, main veins and cells close to them retain chlorophyll longer than other leaf areas (Quirino *et al*. 2000; Fig. 2a), a common senescence strategy also in other species (e.g. Wingler *et al*. 2005; Niewiadomska *et al*. 2009; Wojciechowska *et al*. 2018; Dani *et al*. 2022), which may help to ensure efficient nutrient resorption. However, a different strategy is utilized by maple, as well as by some other species (e.g. Keskitalo *et al*. 2005), suggesting that there are multiple viable ways to senesce (see also Krupinska *et al*. 2012). An increase in photochemical quenching, observed in all leaves after a high-light treatment (Figs. 2–3), may be an indication of an oxidized plastoquinone pool, resulting from reduced amount of functional PSII units.

In both maple and birch, the F_O values measured from green and senescing leaves were similar (Figs. 2–3), despite the latter ones having much lower chlorophyll contents. While the PSII antenna (LHCII) may partly stay undegraded until late senescence, PSII-LHCII-supercomplexes disappear early during autumn senescence in maple (Moy *et al*. 2015; Rantala *et al*. 2023). This might suggest that the detachment of PSII antenna increases the F_O and F_M fluorescence yields and thereby lowers the F_V/F_M values of senescing leaves. However, 77K chlorophyll fluorescence spectrum (reflecting the antenna compositions of PSII and PSI) measured from ground birch leaves did not show an increase in 680 nm emission in senescing leaves (Mattila *et al*. 2021), indicating that if senescence leads to detachment of antenna complexes from the reaction centres, the detached complexes have a low fluorescence yield. On the other hand, the decreased recovery capacity of senescing leaves, as

compared to that of green leaves (Figs. 1–3), may lead to net photoinhibition, possibly increasing the F_O level and, consequently, decreasing F_V/F_M.

Here, senescing leaves showed low NPQ (Figs. 2–3), an observation made also in earlier studies of deciduous (Junker and Ensminger 2016; Mattila *et al*. 2021; Rantala *et al*. 2023) and also other species (e.g. Wingler *et al*. 2004). Low content of PSII and/or (functional) PSII antenna in senescing leaves (Lepeduš *et al*. 2010; Moy *et al*. 2015; Rantala *et al*. 2023) may explain the results. On the other hand, NPQ may also increase during autumn senescence (Mattila and Tyystjärvi 2023). Also here, NPQ, if measured right after switching on an actinic light (at 1.1 min), was high especially in senescing birch leaves (Fig. 2). Accordingly, Wingler *et al*. (2004), who also generally observed low NPQ in senescing leaves of *Arabidopsis thaliana*, reported that some parts of senescing leaves showed high levels of NPQ. Furthermore, the high light treatment and the subsequent recovery affected NPQ differently, if the NPQ was measured after 1.1 min of an actinic illumination or after 3.6 min; at the later time-point NPQ decreased after high light and then again increased while NPQ at the earlier time-point further decreased after the recovery (Figs. 2–3). At least part of the decrease after high light may be explained by increased photoinhibitory quenching. Accordingly, in senescing leaves in which recovery from photoinhibition was also weak, NPQ recovered after a low light recovery period only little or not at all. As similar behaviour was not observed at the early NPQ time-point, part of the decrease may also originate from regulation of NPQ. To conclude, the NPQ capacity of senescing leaves is difficult to judge because NPQ capacity may vary both spatially and temporally (during a short-term illumination).

Previous measurements from deciduous species show a decrease in total amounts of the xanthophyll pigments during autumn senescence, while the proportion of zeaxanthin is generally high (García-Plazaola *et al*. 2003). It has been proposed that NPQ and anthocyanin accumulation present compensatory strategies against high light stress (Cooney *et al*. 2018; Yu *et al*. 2021). Accordingly, Moy *et al*. (2015) observed an increase in the amount of the PsbS protein in oak and suggested that the yellow-senescing oak relies on NPQ while the red-senescing sugar maple (*Acer saccharum*) relies on anthocyanin synthesis. Also, the reddest species (*Cornus sanguinea*) studied by García-Plazaola *et al*. (2003) did not show an upregulation of zeaxanthin that was observed in all other studied species. Here, NPQ did not increase in senescing maple leaves (capable of synthetizing anthocyanins during autumn) in the early measurement point (at 1.1 min after switching on an actinic light) as it did in birch (which does not turn red during autumn) (Figs. 2–3). Unfortunately, it is not known whether the PsbS protein or zeaxanthin are upregulated during autumn senescence in birch. However, we observed an increase in xanthophyll pigments (on chlorophyll basis; Fig. 4c–d;

Table S1) in red senescing leaves of maple but not in yellow senescing leaves. Furthermore, despite differences in xanthophyll pigments, no difference was observed in NPQ between yellow and red parts of senescing leaves. Previously, we have observed more NPQ (as well as other stress symptoms, such as low F_V/F_M values) in red maple leaves than in yellow maple leaves (Mattila and Tyystjärvi 2023). Also here, the red maple leaves showed lower F_V/F_M values than yellow leaves (Fig. 3; Table 1). It should be noted, however, that the red leaves used here contained less chlorophyll than yellow leaves (Table 1), which may have exaggerated the differences, as the F_V/F_M values tend to further decrease when senescence proceeds. Low F_V/F_M values have been observed also in other species with red leaves (Nikiforou *et al.* 2011). To conclude, an inverse relationship between anthocyanins and NPQ does not seem to be a universal phenomenon in autumn leaves.

High carotenoid and α-tocopherol content lower the production of reactive oxygen species in red senescing maple leaves

Thylakoids isolated from senescing maple leaves, especially those isolated from red leaves, contained more α-tocopherol and carotenoids than thylakoids isolated from green leaves (Fig. 4a,b). Here, the antioxidants were quantified on chlorophyll basis, and therefore, it is unclear if the antioxidants increased in senescing leaves, or if their degradation was just slower than that of chlorophyll. Chlorophyll contents of yellow and red senescing leaves, used for the thylakoid isolation, were ~30% and ~20% of that of green leaves (Table 1). Assuming a similar original chlorophyll content, senescing yellow and red leaves contained ~60% and ~75% of their original carotenoid contents, respectively, and ~80% and ~130% of their original α-tocopherol content, respectively. Based on this estimation, only α-tocopherol in red leaves increased during senescence. The calculation agrees with previous literature, as slow degradation of carotenoids (compared to degradation of chlorophyll) has been observed in several deciduous species during autumn senescence while synthesis of tocopherols, especially during early senescence, has been reported (Rise *et al*. 1989; García-Plazaola *et al*. 2003; Szymańska and Kruk 2008; Junker and Ensminger 2016). The high tocopherol content of senescing leaves (Szymańska and Kruk 2008) speaks for the importance of tocopherols for these leaves.

Carotenoids and tocopherols are efficient quenchers and scavengers of singlet oxygen (for a review, see Khorobrykh *et al*. 2020) and thus, we suggest that the low singlet oxygen production in thylakoids isolated from red senescing leaves (Fig. 4e) was due to the high content of carotenoids and α-tocopherol (Fig. 4a,b). In addition, tocopherols can scavenge lipid radicals (Mesa and Munné-Bosch 2023), which may explain the previously detected low amounts of carbon-centered radicals in thylakoids isolated from senescing maple leaves (Rantala *et al*. 2023). Based on our present and

previous results (Fig. 4e; Rantala *et al*. 2023), it can be speculated that thylakoids of senescing leaves are not a significant source of reactive oxygen species during autumn senescence of maple. However, that might still be the case in different species or in different types of senescence (Springer *et al*. 2015; Krieger-Liszkay *et al*. 2015). It should be also noted that the photosynthetic electron transport chain remains highly reduced in isolated thylakoids during an illumination treatment, due to lack of electron sinks (e.g. carbon fixation) and, consequently, the production rates of reactive oxygen species may differ between isolated thylakoids and intact leaves (e.g. Mattila *et al*. 2020; 2023).

Despite the high antioxidant content, thylakoids isolated from senescing leaves were photoinhibited at similar rates as thylakoids isolated from green leaves (Fig. 4f). Similarly, even though singlet oxygen may be important in photoinhibition of PSII (e.g. Vass 2012; Davis *et al*. 2016; Mattila *et al*. 2023), addition of antioxidants does not always protect isolated thylakoids from photodamage (Mattila *et al*. 2023). Furthermore, the reduction state of the photosynthetic electron transport chain does not seem to determine the rate of the damaging reaction of photoinhibition (Hakala *et al*. 2005; Mattila *et al*. 2023); the presence of an artificial electron acceptor during illumination of isolated thylakoid membranes has even been shown to slightly boost photoinhibition instead of offering protection (Hakala *et al*. 2005). The present data show that thylakoids isolated from senescing leaves are not intrinsically more vulnerable against PSII photodamage than those of green leaves (Fig. 4f), but the high rates of photoinhibition observed in senescing leaves (Figs. 1–3; Mattila *et al*. 2021) may indeed derive from the low chlorophyll content of these leaves (Fig. S4; Pätsikkä *et al*. 2002; Serôdio and Campbell 2021).

Isolated thylakoids possess no recovery capacity. In *A. thaliana* leaves, removal of singlet oxygen improves recovery, especially in a tocopherol-less mutant (Hakala-Yatkin *et al*. 2011). Here, we observed no significant differences in the recovery capacity between yellow and red leaf sections of senescing maple (Fig. 3) but, previously, senescing leaves of a highly pigmented garden maple showed very poor recovery (Rantala *et al*. 2023). Thus, the connection between antioxidants and recovery from PSII damage requires further studies in senescing leaves.

Slow repair of PSII at low temperatures may explain low F_V/F_M values during late autumn in senescing birch leaves

F_V/F_M values of senescing birch leaves collected during early autumn were higher than those measured from leaves with a similar chlorophyll content (indicating a similar phase of senescence) but collected during late autumn (Fig. 1a,d). Net photoinhibition is determined by the balance

between the rates of the damage and the repair (for reviews, see Murata *et al*. 2007; Tyystjärvi 2013) and thus, the observed chronic photoinhibition in these leaves may derive either from an increased rate of the damaging reaction or from a decreased rate of the repair reactions. Leaves collected from a single tree at different times during the autumn were photoinhibited at a similar rate and also possessed similar recovery capacities, at laboratory conditions (Fig. 1c–e). However, repair clearly slowed down when temperature was lowered (Fig. 1f–h). Indeed, synthesis of the new D1-protein is known to slow down at low temperatures (Greer *et al*. 1986; Grennan and Ort 2007). The rate of the damaging reaction of photoinhibition, on the other hand, has been shown to decrease with decreasing temperature (Mattila *et al*. 2020; Mattila *et al*. 2023). Weather during late autumn is usually colder than during early autumn (e.g. Fig. 1b) and therefore, we suggest that low temperatures during late autumn slow down the repair reactions, which leads to an accumulation of non-functional PSII units in senescing leaves. Previously, we observed large, reversible drops in PSII functionality after cold (below-zero) nights during autumn, both in senescing and green maple leaves (Mattila and Tyystjärvi 2023); inhibition of the repair reactions by low temperatures may explain also these observations.

Senescing leaves have also previously been shown to recover from photoinhibition, albeit weakly (Mattila *et al*. 2021; Mattila and Tyystjärvi 2023). The fluorescence imaging revealed that only the green parts of senescing birch leaves recovered (Fig. 2). Similarly, some areas in senescing maple leaves showed no recovery (see Fig. 3n), although in general more recovery was observed in senescing maple than in senescing birch. Senescence of a leaf lasts from one to two weeks (Mattila *et al*. 2018; Mattila and Tyystjärvi 2023), but it is not known, to our knowledge, for how long it takes for a cell or a chloroplast to senesce. It can be speculated, therefore, that the recovery observed in senescing leaves derives only from those cells that have not yet started to senesce, but further studies are needed to test this hypothesis.

Conflicts of interests

The authors declare no conflicts of interest.

Data availability statement

Data will be available upon request from the authors.

Acknowledgements

Riina Aitokari is thanked for optimizing the thylakoid isolation and for isolating a set of thylakoids.

Declaration of funding

The work was supported by the Ella and Georg Ehrnrooth Foundation, the Osk. Huttunen Foundation and the Research Council of Finland (project 333421).

References

Agati G, Guidi L, Landi M, Tattini M (2021) Anthocyanins in photoprotection: knowing the actors in play to solve this complex ecophysiological issue. *New Phytologist* 232, 2228–2235.

Anderson R, Ryser P (2015) Early autumn senescence in red maple (*Acer rubrum* L.) is associated with high leaf anthocyanin content. *Plants (Basel)* 4, 505–22.

Cheeseman JM (2009) Seasonal patterns of leaf H2O2 content: reflections of leaf phenology, or environmental stress? *Functional Plant Biology* 36, 721–731.

Cooney LJ, Logan BA, Walsh MJL, Nnatubeugo NB, Reblin JS, Gould KS (2018) Photoprotection from anthocyanins and thermal energy dissipation in senescing red and green Sambucus canadensis peduncles. *Environmental and Experimental Botany* 148, 27–34.

Dani KGS, Pollastri S, Pinosio S, Reichelt M, Sharkey TD, Schnitzler JP, Loreto F (2022) Isoprene enhances leaf cytokinin metabolism and induces early senescence. *New Phytologist* 234, 961–974.

Davis GA, Kanazawa A, Schöttler MA, Kohzuma K, Froehlich JE, Rutherford AW, Satoh-Cruz M, Minhas D, Tietz S, Dhingra A, Kramer DM (2016) Limitations to photosynthesis by proton motive force-induced photosystem II photodamage. *Elife* 5, e16921.

Dodge JD (1970) Changes in chloroplast fine structure during the autumnal senescence of *Betula* leaves. *Annals of Botany* 34, 817–824.

García-Plazaola JI, Hernández A, Becerril JM (2003) Antioxidant and pigment composition during autumnal leaf senescence in woody deciduous species differing in their ecological traits. *Plant Biology (Stuttg)* 5, 557–566.

Greer DH, Berry JA, Björkman O (1986) Photoinhibition of photosynthesis in intact bean leaves: role of light and temperature, and requirement for chloroplast-protein synthesis during recovery. *Planta* 168, 253–260.

Grennan AK, Ort DR (2007) Cool temperatures interfere with D1 synthesis in tomato by causing ribosomal pausing. *Photosynthesis Research* 94, 375–385.

Hakala M, Tuominen I, Keränen M, Tyystjärvi T, Tyystjärvi E (2005) Evidence for the role of the oxygen-evolving manganese complex in photoinhibition of Photosystem II. *Biochimica et Biophysica Acta* 1706, 68–80.

Hakala-Yatkin M, Sarvikas P, Paturi P, Mäntysaari M, Mattila H, Tyystjärvi T, Nedbal L, Tyystjärvi E (2011) Magnetic field protects plants against high light by slowing down production of singlet oxygen. *Physiologia Plantarum* 142, 26–34.

Hughes NM, George CO, Gumpman CB, Neufeld HS (2022) Coevolution and photoprotection as complementary hypotheses for autumn leaf reddening: a nutrient-centered perspective. *New Phytologist* 233, 22–29.

Hunt RE, Daughtry CST (2014) Chlorophyll meter calibrations for chlorophyll content using measured and simulated leaf transmittances. *Agronomy Journal* 106, 931–939.

Junker LV, Ensminger I (2016) Relationship between leaf optical properties, chlorophyll fluorescence and pigment changes in senescing *Acer saccharum* leaves. *Tree Physiology* 36, 694–711.

Keskitalo J, Bergquist G, Gardeström P, Jansson S (2005) A cellular timetable of autumn senescence. *Plant Physiology* 139, 1635–1648.

Khorobrykh S, Havurinne V, Mattila H, Tyystjärvi E (2020) Oxygen and ROS in photosynthesis. *Plants* 9, 91.

Kitao M, Yazaki K, Tobita H, Agathokleous E, Kishimoto J, Takabayashi A, Tanaka R (2022) Exposure to strong irradiance exacerbates photoinhibition and suppresses N resorption during leaf senescence in shade-grown seedlings of fullmoon maple (*Acer japonicum*). *Frontiers in Plant Science* 13, 1006413.

Kramer DM, Johnson G, Kiirats O, Edwards GE (2004) New flux parameters for the determination of QA redox state and excitation fluxes. *Photosynthesis Research* 79, 209–218.

Krieger-Liszkay A, Krupinska K, Shimakawa G (2019) The impact of photosynthesis on initiation of leaf senescence. *Physiologia Plantarum* 166, 148–164.

Krieger-Liszkay A, Trösch M, Krupinska K (2015) Generation of reactive oxygen species in thylakoids from senescing flag leaves of the barley varieties Lomerit and Carina. *Planta* 241, 1497–1508.

526 Krupinska K, Mulisch M, Hollmann J, Tokarz K, Zschiesche W, Kage H, Humbeck K, Bilger W
527 (2012) An alternative strategy of dismantling of the chloroplasts during leaf senescence observed in
528 a high-yield variety of barley. *Physiologia Plantarum* 144, 189–200.

529 Kuai B, Chen J, Hörtensteiner S (2018) The biochemistry and molecular biology of chlorophyll
530 breakdown. *Journal of Experimental Botany* 69, 751–767.

531 Lehtimäki N, Shunmugam S, Jokela J, Wahlsten M, Carmel D, Keränen M, Sivonen K, Aro EM,
532 Allahverdiyeva Y, Mulo P (2011) Nodularin uptake and induction of oxidative stress in spinach
533 (*Spinachia oleracea*). *Journal of Plant Physiology* 168, 594–600.

534 Lepeduš H, Jurković V, Štolf I, Ćurković-Peric M, Fulgosi H, Cesar V (2010) Changes in
535 photosystem II photochemistry in senescing maple leaves. *Croatica Chemica Acta* 83, 379–386.

536 Lev-Yadun S (2022) The phenomenon of red and yellow autumn leaves: hypotheses, agreements
537 and disagreements. *Journal of Evolutionary Biology* 35, 1245–1282.

538 Lihavainen J, Edlund E, Björkén L, Bag P, Robinson KM, Jansson S (2021) Stem girdling affects
539 the onset of autumn senescence in aspen in interaction with metabolic signals. *Physiologia*
540 *Plantarum* 172, 201–217

541 Mattila H, Mishra KB, Kuusisto I, Mishra A, Novotná K, Šebela D, Tyystjärvi E (2020) Effects of
542 low temperature on photoinhibition and singlet oxygen production in four natural accessions of
543 Arabidopsis. *Planta* 252, 19.

544 Mattila H, Valev D, Havurinne V, Khorobrykh S, Virtanen O, Antinluoma M, Mishra KB,
545 Tyystjärvi E (2018) Degradation of chlorophyll and synthesis of flavonols during autumn
546 senescence –The story told by individual leaves. *Annals of Botany PLANTS* 10, ply028.

547 Mattila H, Tyystjärvi E (2023) Red pigments in autumn leaves of Norway maple do not offer
548 significant photoprotection but coincide with stress symptoms. *Tree Physiology* 43, 751–768.

549 Mattila H, Sotoudehnia P, Kuuslampi T, Stracke R, Mishra KB, Tyystjärvi E (2021) Singlet
550 oxygen, flavonols and photoinhibition in green and senescing silver birch leaves. *Trees - Structure*
551 *and Function* 35, 1267–1282.

552 Mattila H, Mishra S, Tyystjärvi T, Tyystjärvi E (2023) Singlet oxygen production by Photosystem
553 II is caused by misses of the oxygen evolving complex. *New Phytologist* 237, 113–125.

554 Mesa T, Munné-Bosch S (2023) α-Tocopherol in chloroplasts: Nothing more than an antioxidant?
555 *Current Opinion in Plant Biology* 74, 102400.

556 Moy A, Le S, Verhoeven A (2015) Different strategies for photoprotection during autumn
557 senescence in maple and oak. *Physiologia Plantarum* 155, 205–216.

558 Murata N, Takahashi S, Nishiyama Y, Allakhverdiev SI (2007) Photoinhibition of photosystem II
559 under environmental stress. *Biochimica et Biophysica Acta (BBA) - Bioenergetics* 1767, 414–421.

560 Niewiadomska E, Polzien L, Desel C, Rozpadek P, Miszalski Z, Krupinska K (2009) Spatial
561 patterns of senescence and development-dependent distribution of reactive oxygen species in
562 tobacco (*Nicotiana tabacum*) leaves. *Journal of Plant Physiology* 166, 1057–1068.

563 Nikiforou C, Nikopoulos D, Manetas Y (2011) The winter-red-leaf syndrome in *Pistacia lentiscus*:
564 evidence that the anthocyanic phenotype suffers from nitrogen deficiency, low carboxylation
565 efficiency and high risk of photoinhibition. *Journal of Plant Physiology* 168, 2184–2187.

566 Oxborough K, Baker NR (1997) Resolving chlorophyll a fluorescence images of photosynthetic
567 efficiency into photochemical and nonphotochemical components—calculation of qP and Fv'/Fm'
568 without measuring Fo'. *Photosynthesis Research* 54, 135–142.

569 Pätsikkä E, Kairavuo M, Šeršen F, Aro EM, Tyystjärvi E (2002) Excess copper predisposes
570 photosystem II to photoinhibition in vivo by outcompeting iron and causing decrease in leaf
571 chlorophyll. *Plant Physiology* 129, 1359–1367.

572 Porra RJ, Thompson WA, Kriedemann PE (1989) Determination of accurate extinction coefficients
573 and simultaneous equations for assaying chlorophylls a and b extracted with four different solvents:
574 verification of the concentration of chlorophyll standards by atomic absorption spectroscopy.
575 *Biochimica et Biophysica Acta* 975, 384–394.

576 Quirino BF, Noh YS, Himmelblau E, Amasino RM (2000) Molecular aspects of leaf senescence.
577 *Trends in Plant Science* 5, 278–282.

578 Rantala M, Mulo P, Tyystjärvi E, Mattila H (2023) Biophysical and molecular characteristics of
579 senescing leaves of two Norway maple varieties differing in anthocyanin content. *Physiologia*
580 *Plantarum* 175, e13999.

581 Renner SS, Zohner CM (2019) The occurrence of red and yellow autumn leaves explained by
582 regional differences in insolation and temperature. *New Phytologist* 224, 1464–1471.

583 Rise M, Cojocaru M, Gottlieb HE, Goldschmidt EE (1989) Accumulation of α-tocopherol in
584 senescing organs as related to chlorophyll degradation. *Plant Physiology* 89, 1028–1030.

585 Ruberti C, Barizza E, Bodner M, La Rocca N, De Michele R, Carimi F, Lo Schiavo F, Zottini M
586 (2014) Mitochondria change dynamics and morphology during grapevine leaf senescence. *PLoS*
587 *ONE* 9, e102012.

588 Sasi JM, Gupta S, Singh A, Kujur A, Agarwal M, Katiyar-Agarwal S (2022) Know when and how
589 to die: gaining insights into the molecular regulation of leaf senescence. *Physiology and Molecular*
590 *Biology of Plants* 28, 1515–1534.

591 Serôdio J, Campbell DA (2021) Photoinhibition in optically thick samples: Effects of light
592 attenuation on chlorophyll fluorescence-based parameters. *Journal of Theoretical Biology* 513,
593 110580.

594 Shi D, Wei X, Chen G, Xu Y (2012) Changes in photosynthetic characteristics and antioxidative
595 protection in male and female ginkgo during natural senescence. *Journal of American Society of*
596 *Horticultural Sciences* 137, 349–360.

597 Springer A, Acker G, Bartsch S, Bauerschmitt H, Reinbothe S, Reinbothe C (2015) Differences in
598 gene expression between natural and artificially induced leaf senescence in barley. *Journal of Plant*
599 *Physiology* 176, 180–191.

600 Szymańska R, Kruk J (2008) Tocopherol content and isomers' composition in selected plant
601 species. *Plant Physiology and Biochemistry* 46, 29–33.

602 Tyystjärvi E. (2013) Photoinhibition of photosystem II. *International Review of Cell and Molecular*
603 *Biology* 300, 243–303.

604 Uzarević Z, Štolfa I, Parađiković N, Cesar V (2011) Physiology and biochemistry of leaf bleaching
605 in prematurely aging maple (*Acer saccharinum* L.) trees: I. Hydrogen peroxide level, antioxidative
606 responses and photosynthetic pigments. *Acta Botanica Croatica* 70, 121–132

607 Vass I (2012) Molecular mechanisms of photodamage in the photosystem II complex. *Biochimica*
608 *et Biophysica Acta* 1817, 209–217.

609 Wellburn AR (1994) The spectral determination of chlorophylls a and b, as well as total
610 carotenoids, using various solvents with spectrophotometers of different resolution. *Journal of*
611 *Plant Physiology* 144, 307–313.

612 Wingler A, Brownhill E, Pourtau N (2005) Mechanisms of the light-dependent induction of cell
613 death in tobacco plants with delayed senescence. *Journal of Experimental Botany* 56, 2897–2905.

614 Wingler A, Marès M, Pourtau N (2004) Spatial patterns and metabolic regulation of photosynthetic
615 parameters during leaf senescence. *New Phytologist* 161, 781–789.

616 Wojciechowska N, Marzec-Schmidt K, Kalemba EM, Zarzyńska-Nowak A, Jagodziński AM,
617 Bagniewska-Zadworna A (2018) Autophagy counteracts instantaneous cell death during seasonal
618 senescence of the fine roots and leaves in *Populus trichocarpa*. *BMC Plant Biology* 18, 260.

619 Yu ZC, Lin W, Zheng XT, Chow WS, Luo YN, Cai ML, Peng CL (2021) The relationship
620 between anthocyanin accumulation and photoprotection in young leaves of two dominant tree
621 species in subtropical forests in different seasons. *Photosynthesis Research* 149, 41–55.

Figures

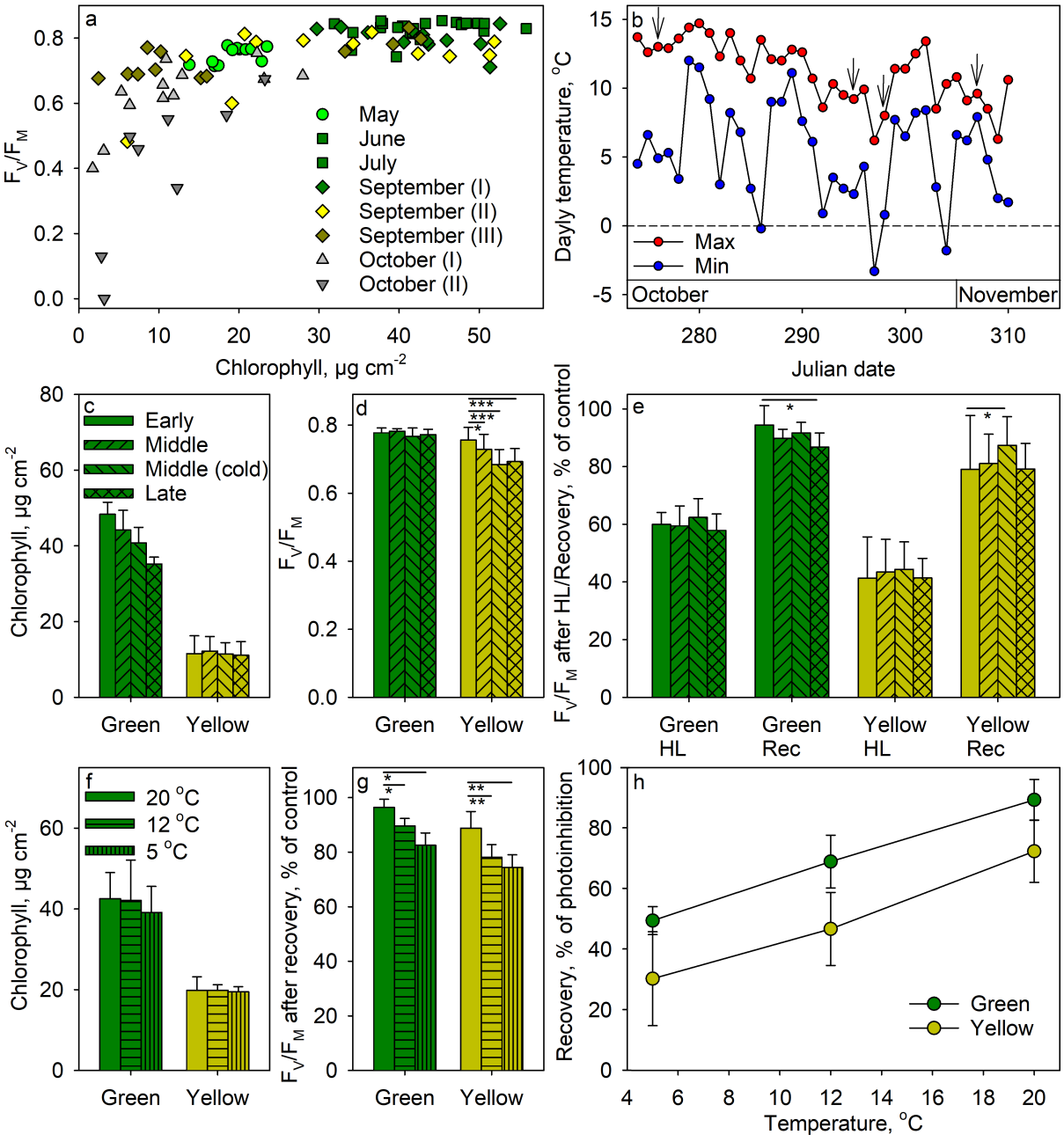

Figure 1. PSII activity and photoinhibition in birch leaves collected during spring, summer and autumn. (a) F_V/F_M values measured from leaves with different chlorophyll contents, collected on 27/5/2020 (May), 25/6/2020 (June), 28/7/2020 (July), 1/9/2020 (September I), 14/9/2020 (September II), 23/9/2020 (September III), 13/10/2020 (October I) and 20/10/2020 (October II). The symbols represent individual measurements on leaves, collected from three individual trees. (b) Daily maximum (red circles) and minimum (blue circles) temperatures during autumn 2022. The arrows highlight the collection dates for the leaves used in (c–e); 3/10/2022 (early), 22/10/2022

631 (middle), 25/10/2022 (middle, cold) and 3/11/2022 (late). (c) Chlorophyll contents, (d) control
632 F_V/F_M values and (e) F_V/F_M values (as percentages of the control) after 1 h of high light (HL; PPFD
633 2000 µmol m^{-2} s^{-1}) and after 4 h of recovery (Rec; PPFD ~15 µmol m^{-2} s^{-1}) both at 20°C, of non-
634 senescing (green) and senescing (yellow) leaves, collected during early, middle (before and after a
635 cold night) and late phases of autumn senescence from a single tree (see Fig. S3). (f) Chlorophyll
636 contents and (g) F_V/F_M values (as percentages of the control) after 1 h of high light (at 20°C, PPFD
637 2000 µmol m^{-2} s^{-1}) and after 4 h of recovery (PPFD ~15 µmol m^{-2} s^{-1}) at the indicated temperatures
638 (5, 12 or 20°C) of non-senescing (green) and senescing (yellow) leaves, collected on 20–26/9/2023.
639 (h) Percentage of the photoinhibition (decrease in F_V/F_M after high light) that was recovered,
640 calculated based on (g), as a function of recovery temperature. F_V/F_M values have been measured
641 after 30 min in darkness (at 20°C). Bars represent average values and error bars SD, calculated
642 based on 3–4 (green) or 4–12 (yellow) measurements on individual leaves, collected from at least
643 three individual trees, except in (c–e) where the leaves are from a single tree. Statistically
644 significant differences between the indicated groups are highlighted with asterisks.

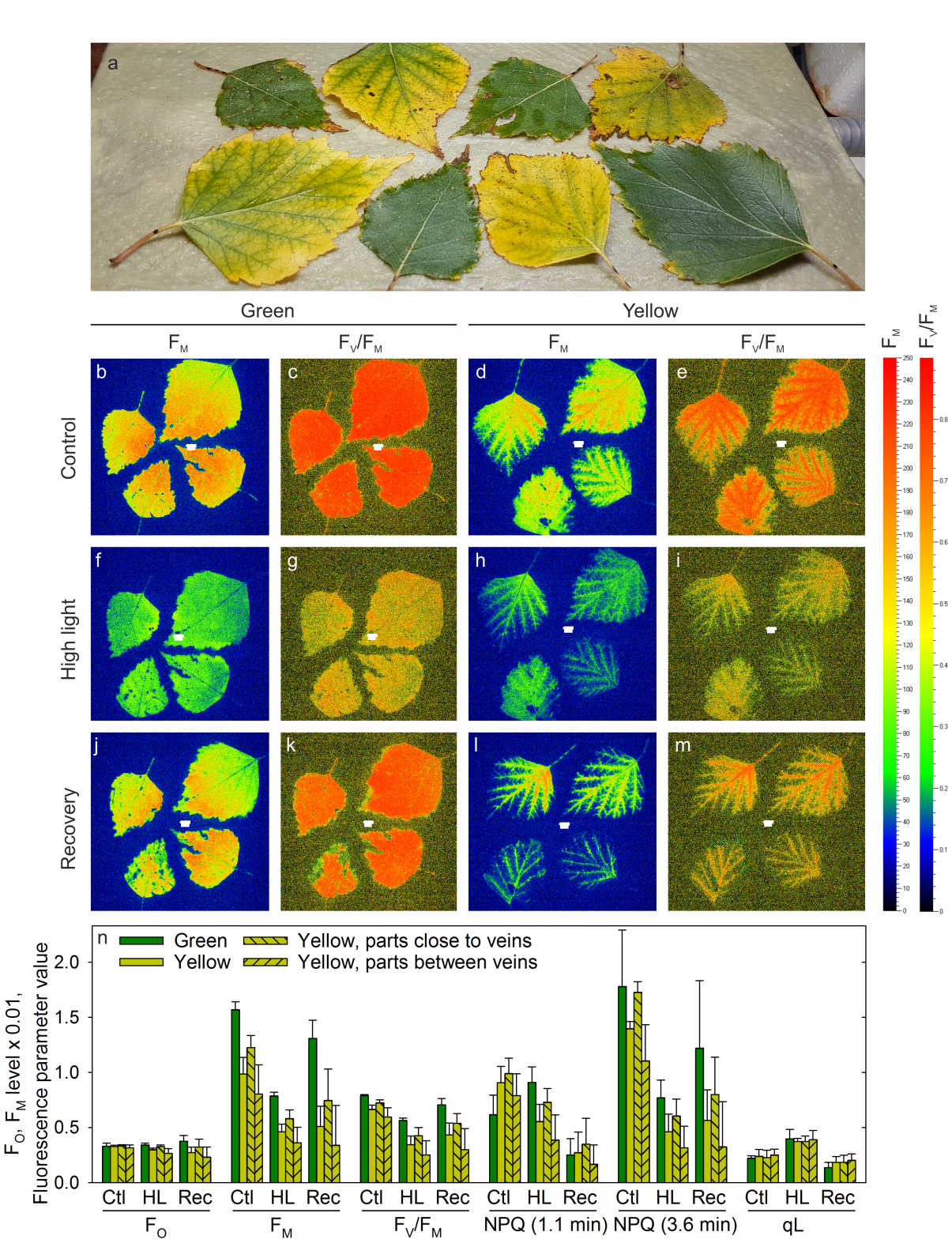

645

646 Figure 2. Chlorophyll *a* fluorescence imaging on non-senescing (green) and senescing (yellow)
647 birch leaves, collected on 14/10/2020. (a) A photograph of the leaves. (b–m) Examples of false-
648 coloured, otherwise untreated, fluorescence images taken from dark-acclimated (> 30 min) leaves;
649 maximal fluorescence F_M (b, d, f, h, j, l) and the fluorescence parameter F_V/F_M (c, e, g, i, k, m).

Scale bars are in the right. After the first fluorescence imaging (Control; b–e), green leaves were illuminated for 4 h and yellow leaves for 2 h (PPFD 1300 µmol m^{-2} s^{-1}), dark-acclimated (> 30 min) and re-imaged (High light; f–i). Finally, leaves were let to recover over-night (14 h) under low light (PPFD ~10 µmol m^{-2} s^{-1}), dark-acclimated (> 30 min) and imaged again (Recovery; j–m). (n) Quantification of the measurements. In the case of yellow leaves, in addition to the fluorescence values averaged over the whole leaf, leaf parts close to main veins and leaf parts between veins were analysed separately (see Fig. S2). F_O = minimum fluorescence. qL and NPQ were calculated after illuminating the leaves with an actinic light (red light of PPFD ~265 µmol m^{-2} s^{-1}) and firing additional saturating pulses at the indicated times. Ctl = Control, HL = After high light, Rec = After recovery. Bars show averages and error bars show SD, calculated based on imaging of four individual leaves collected from four trees. See Fig. S5 for the original fluorescence traces.

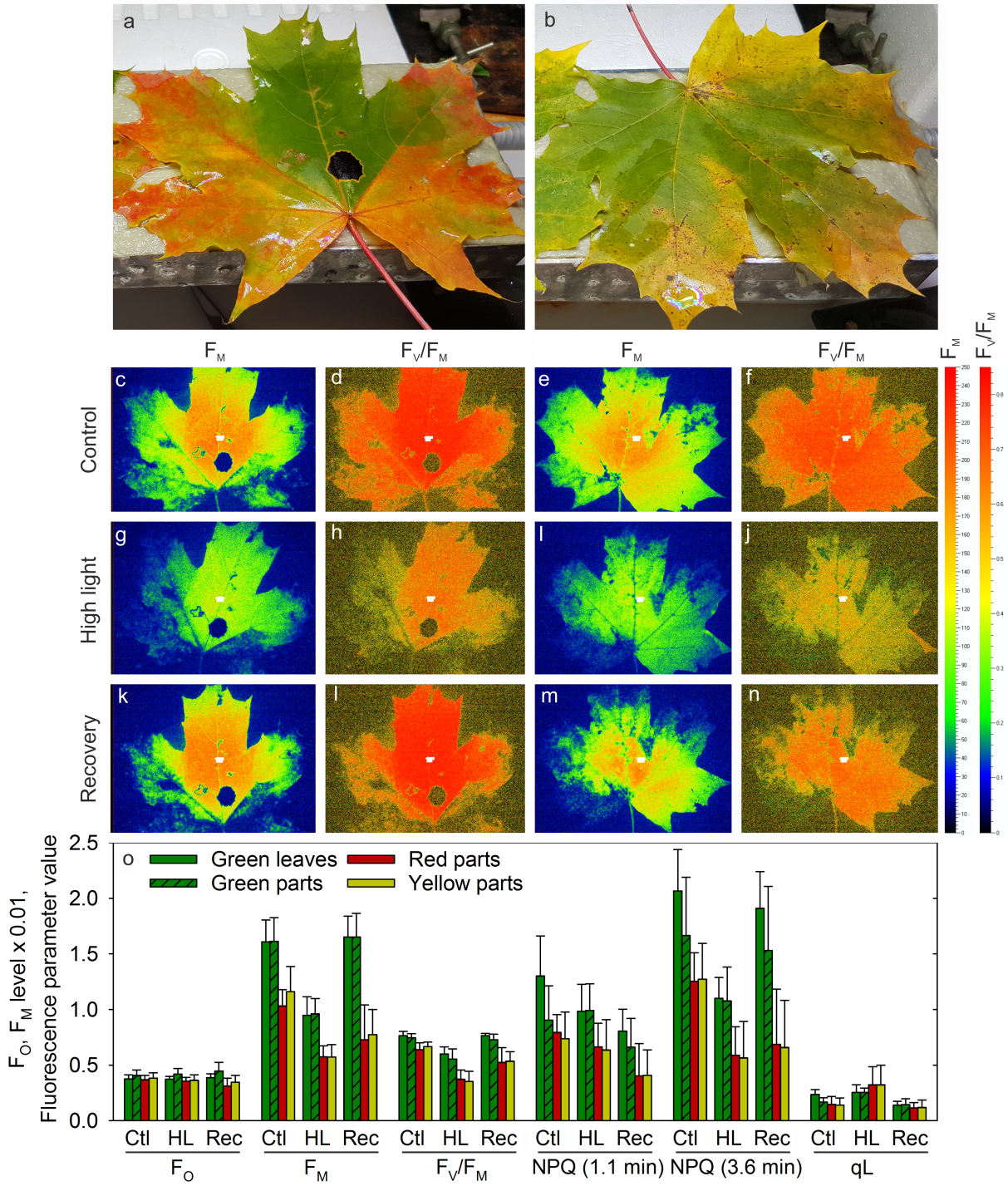

Figure 3. Chlorophyll *a* fluorescence imaging on non-senescing (green) and senescing (containing green, red and yellow sections) maple leaves, collected on 12–19/10/2020. (a–b) Examples of the leaves. (c–n) Examples of false-coloured, otherwise untreated, fluorescence images taken from dark-acclimated (> 30 min) leaves; maximal fluorescence F_M (c, e, g, i, k, m) and the fluorescence parameter F_V/F_M (d, f, h, j, l, n). Scale bars are in the right. After the first fluorescence imaging (Control; c–f), leaves were illuminated for 2 h (PPFD 1300 µmol m^{-2} s^{-1}), dark-acclimated (> 30 min) and re-imaged (High light; g–j). Finally, leaves were let to recover over-night (14 h) under low

light (PPFD ~10 µmol m^{-2} s^{-1}), dark-acclimated (> 30 min) and imaged again (Recovery; k–n). (o) Quantification of the measurements. In the case of senescing leaves, leaf sections were manually annotated as green, yellow or red and analysed separately. F_O = minimum fluorescence. qL and NPQ were calculated after illuminating the leaves with an actinic light (red light of PPFD ~235 µmol m^{-2} s^{-1}) and firing additional saturating pulses at the indicated time points. Ctl = Control, HL = After high light, Rec = After recovery. Bars show averages and error bars show SD, calculated based on imaging of at least three individual leaves collected from at least three trees. See Fig. S6 for the original fluorescence traces.

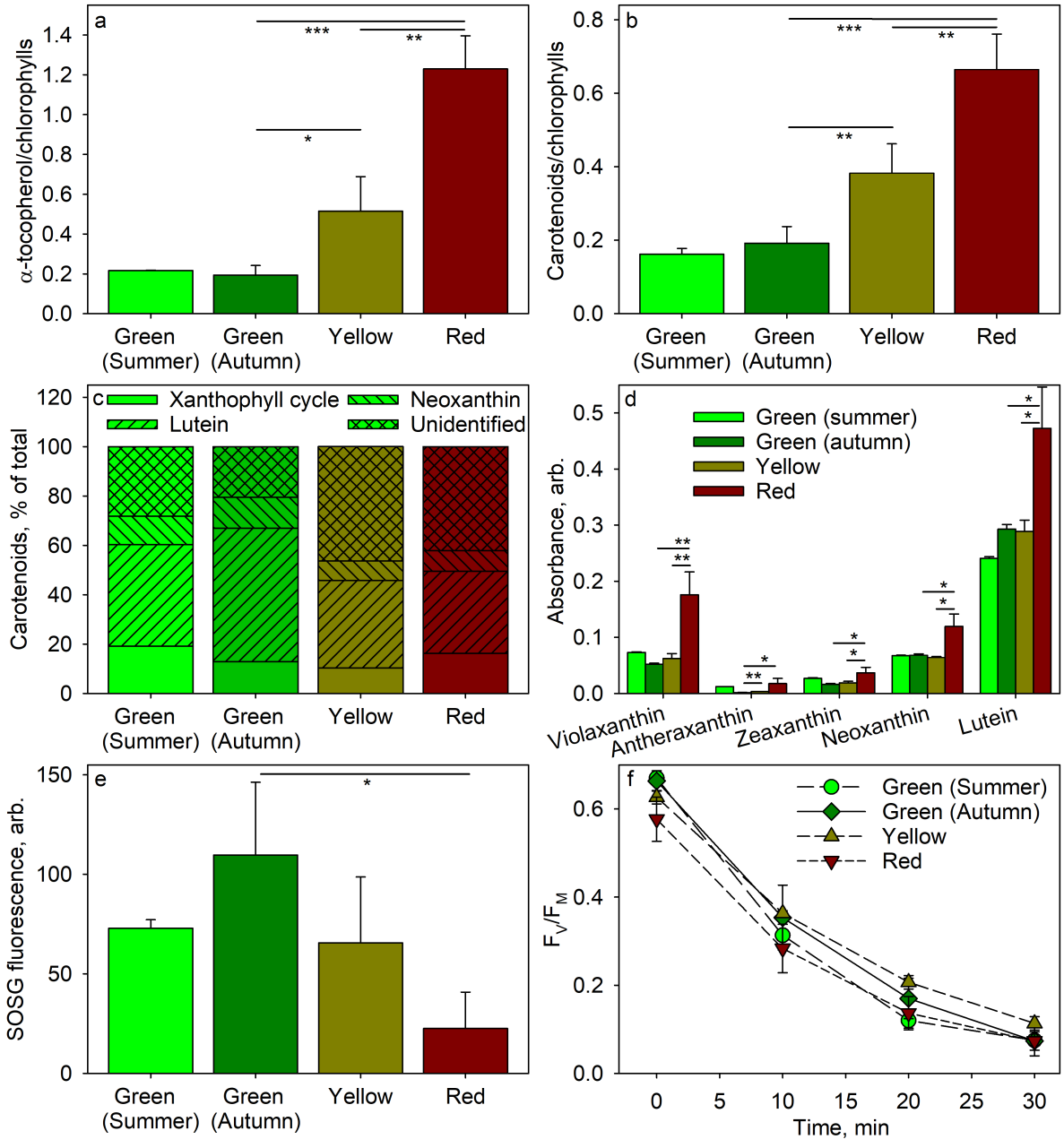

Figure 4. Antioxidants, singlet oxygen and photoinhibition in thylakoids isolated from non-senescing (green) leaves (collected either during summer or autumn, as indicated) and from yellow or red senescing leaves of maple, collected on 15/7/2021 and 24/9/2021–9/10/2021. (a) Ratio of α-tocopherol to total chlorophyll, measured with HPLC. (b) Ratio of carotenoids to total chlorophyll, measured spectrophotometrically. (c) Proportions of the detected carotenoids, measured with HPLC. (d) Amounts of violaxanthin, antheraxanthin, zeaxanthin, neoxanthin and lutein, measured with HPLC. (e) Production of singlet oxygen, detected with SOSG, during a 10 min illumination with red light (PPFD 2000 μmol m^{-2} s^{-1}). (d) Time course of photoinhibition, quantified by the fluorescence parameter F_V/F_M, during illumination with white light (PPFD 2000 μmol m^{-2} s^{-1}). For quantification, see Table 1. The data show averages from at least three independent experiments, and error bars show SD. Statistically significant differences between the indicated groups are highlighted with asterisks. Summer thylakoids have not been compared to the other groups.

Cite this: Mattila H et al. (2024) Both external and internal factors induce heterogeneity in senescing leaves of deciduous trees. Functional Plant Biology 51, FP24012. doi:10.1071/FP24012

Supplementary data:

Both external and internal factors induce heterogeneity in senescing leaves of deciduous trees

Heta Mattila[1,2]*, Sergey Khorobrykh[1], Esa Tyystjärvi[1]

[1]Molecular Plant Biology, University of Turku, Finland

[2]Centre for Environmental and Marine Studies, University of Aveiro, Portugal

*Corresponding author email: h.mattila@ua.pt

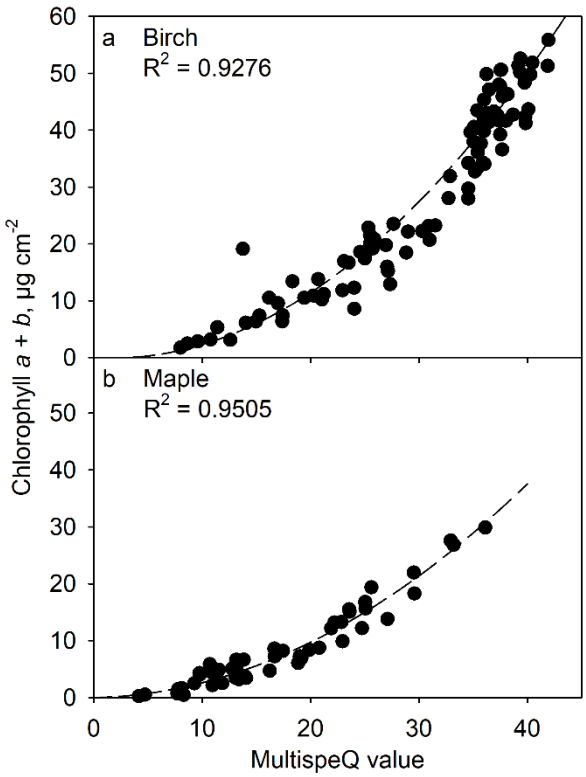

Figure S1. Calibration of optical (SPAD) chlorophyll measurements. Chlorophyll contents of birch (a) and maple (b) leaves were measured first with an optical method (MultispeQ) and then spectrophotometrically after extraction in DMF (Chlorophyll *a* + *b*, µg cm^{-2}). Symbols show individual measurements and lines show second-order polynomial equations fitted to the data (R^2 values of the fits are indicated). See Materials and methods for the equations.

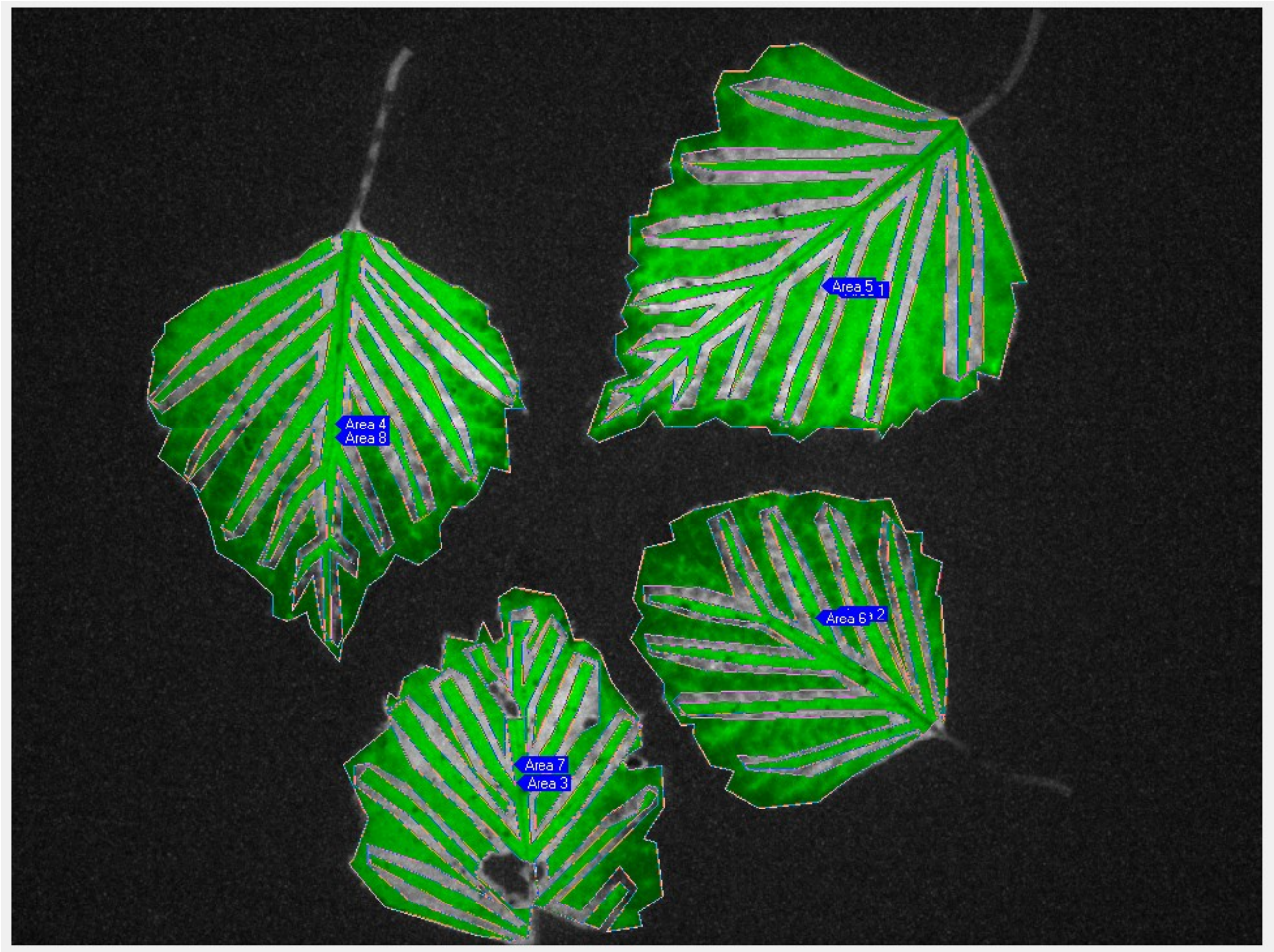

Figure S2. Selected areas of interests for the analysis of chlorophyll *a* fluorescence images from senescing birch leaves for Fig. 2. The underlaying grayscale image shows chlorophyll fluorescence. Black corresponds to background. Manually selected areas of interests are super-imposed on the fluorescence image with green colour and highlighted with blue labels. Two areas of interests are drawn on each leaf; areas close to main veins and areas between the main veins.

Figure S3. Photographs, taken on (a) 3/10/2022, (b) 22/10/2022, (c) 25/10/2022 and (d) 3/11/2022, of a senescing silver birch tree, used for the experiments in Fig. 1c–e. Note that more yellow leaves appear in (a) than in (b) because a slow progression of senescence during the first two dates.

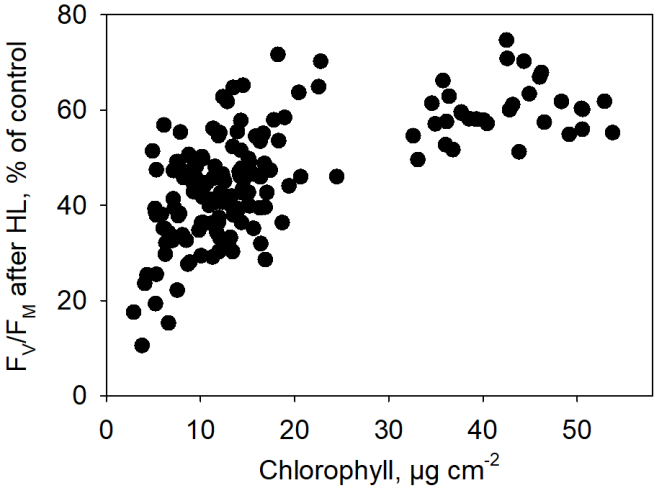

Figure S4. Remaining PSII activities, as percentages of the control (prior an illumination) F_V/F_M values, after a high light treatment (HL) plotted against the chlorophyll content of the leaf. The symbols show individual measurements. The data are from Fig. 1c–e.

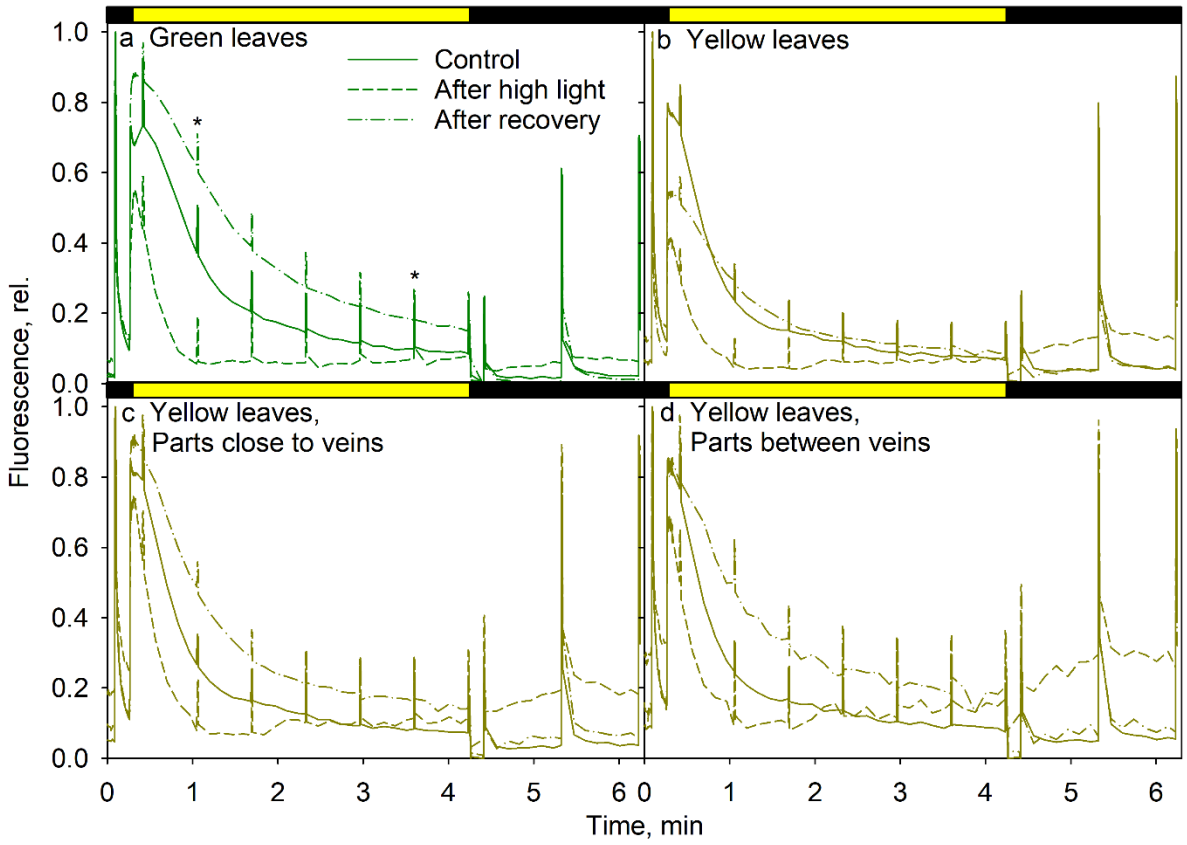

Figure S5. Fluorescence traces measured from green (a) and senescing (yellow; b–d) birch leaves. In the case of yellow leaves, fluorescence values were averaged over whole leaves (b), and also over leaf parts close to main veins (c) and over leaf parts between veins (d). See Fig. S2 for examples. The imaging protocol is shown above the figures; black horizontal bars indicate darkness (only a weak measuring beam on) and the yellow bars indicate actinic illumination (red light of PPFD ~265 µmol m^{-2} s^{-1}). In addition, 10 saturating pulses were fired to calculate F_V/F_M, NPQ and qL; the asterisks in (a) indicate the time points for NPQ measurements (Fig. 2). Before the fluorescence imaging, leaves were kept at least 30 min in the dark. After the control measurements, leaves were illuminated for four (green leaves) or two (yellow leaves) hours (PPFD 1300 µmol m^{-2} s^{-1}; After high light), after which they were let to recover over-night (14 h) under low light (PPFD ~10 µmol m^{-2} s^{-1}; After recovery). Leaves were collected on 14/10/2020, from four birch trees (one green leaf and one yellow leaf per tree). Lines show averages and from four independent measurements.

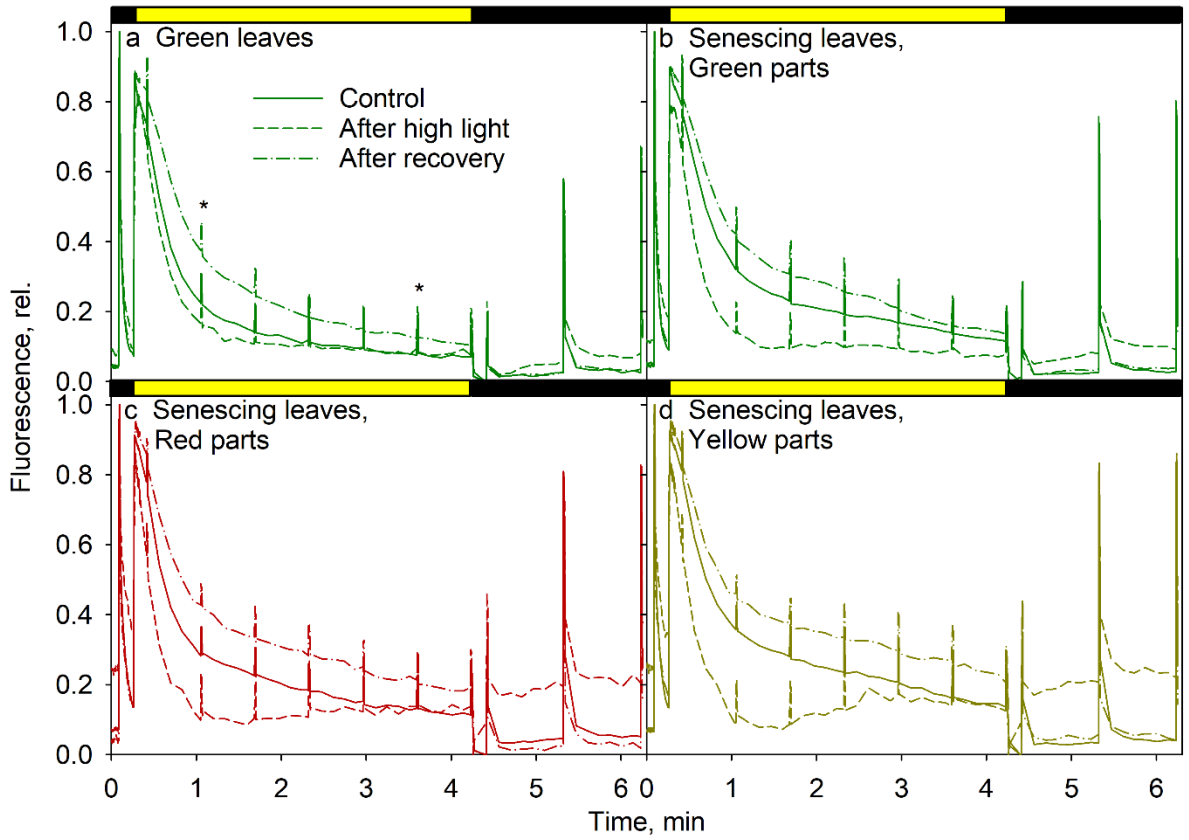

Figure S6. Fluorescence traces measured from green (a) and senescing (b–d) maple leaves. In the case of senescing leaves, leaf sections were manually annotated as green (b), red (c) or yellow (d). The imaging protocol is shown above the figures; black horizontal bars indicate darkness (only a weak measuring beam on) and the yellow bars indicates an actinic illumination (red light of PPFD ~235 µmol m^{-2} s^{-1}). In addition, 10 saturating pulses were fired to calculate F_V/F_M, NPQ and qL; the asterisks in (a) indicate the time points for NPQ measurements (Fig. 3). Before the fluorescence imaging, leaves were kept at least 30 min in the dark. After the control measurements, leaves were illuminated for two hours (PPFD 1300 µmol m^{-2} s^{-1}; After high light), after which they were let to recover over-night (14 h) under low light (PPFD ~10 µmol m^{-2} s^{-1}; After recovery). Leaves were collected on 12–19/10/2020, from three maple trees (one green leaf and at least one senescing leaf per tree). Lines show averages from at least three independent measurements.

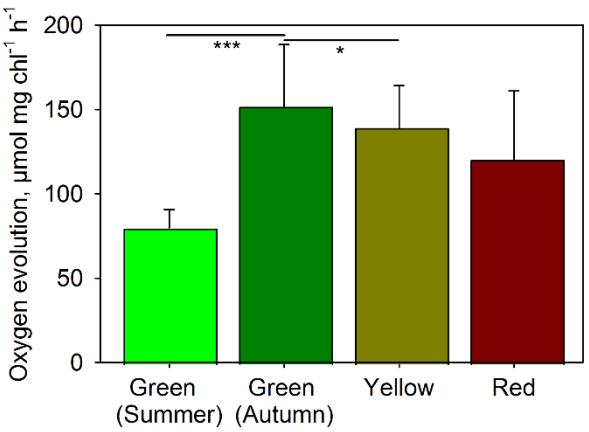

Figure S7. Light-saturated (maximum) oxygen evolution capacity of PSII in the presence of an artificial electron acceptor (0.5 mM 2,6-dimethoxybenzoquinone), measured from thylakoids isolated from fully green leaves (collected either during summer or autumn, as indicated) and from yellow or red senescing leaves of maple. All samples contained the same amount of chlorophyll. Statistically significant differences between the indicated groups are highlighted with asterisks.

Table S1. Retention times and areas (related to chlorophylls) of peaks associated with different carotenoids (recognized based on their absorption spectra), detected with HPLC from thylakoids, isolated from fully green leaves (collected either during summer or autumn, as indicated) and from yellow or red senescing leaves of maple. neo = neoxanthin, vio = violaxanthin, ant = antheraxanthin and zea =zeaxanthin. N.d. = not detected. N.a. = not available.

Peak	**Retention time, min**	**Green (summer)**	**Green (autumn)**	**Yellow**	**Red**	**Yellow, % of Green**	**Red, % of Green**
1	4.1	0.0011	0.0012	0.0019	0.0031	154	248
2	5.8	0.0009	0.0011	0.0012	0.0014	112	123
3	6.5	0.0027	0.0024	0.0028	0.0040	113	164
4	6.7	0.0038	0.0054	0.0070	0.0115	129	211
5 (neo)	7.3	0.0673	0.0681	0.0640	0.1195	94	175
6 (vio)	9.7	0.0732	0.0523	0.0622	0.1759	119	**337**
7	10.7	0.0065	0.0037	0.0074	0.0186	203	**508**
8	11.6	0.0005	0.0007	0.0008	0.0021	117	**320**
9	12.1	0.0022	0.0056	0.0053	0.0117	95	**210**
10 (ant)	12.5	0.0121	0.0015	0.0034	0.0176	228	**1194**
11 (lutein)	13.8	0.2409	0.2928	0.2889	0.4726	99	161
12 (zea)	14.0	0.0156	n.d.	n.d.	0.0145	n.a.	n.a.
13 (zea)	14.2	0.0112	0.0162	0.0190	0.0223	117	138
14	16.1	0.0012	0.0008	0.0018	0.0015	216	182
15	16.3	0.0048	0.0041	0.0036	0.0045	86	108
16	16.5	0.0026	n.d.	n.d.	n.d.	n.a.	n.a.
17	16.7	0.0072	n.d.	n.d.	n.d.	n.a.	n.a.
18	16.9	0.0131	n.d.	n.d.	n.d.	n.a.	n.a.
19 (Chl *b*)	17.3	0.2310	0.2435	0.2170	0.2132	89	88
20	18.1	0.0034	0.0010	0.0240	0.0442	2319	4272
21	18.5	0.0080	0.0004	0.0070	0.0101	1637	2370
22	18.7	0.0022	n.d.	0.0132	0.1123	n.a.	**n.a.**
23 (Chl *a*)	19.0	0.7690	0.7565	0.7830	0.7868	104	104
24	19.3	0.0005	n.d.	0.0066	0.0034	n.a.	n.a.
25	19.5	0.0013	n.d.	0.0030	0.0115	n.a.	**n.a.**
26	19.8	n.d.	n.d.	0.0010	0.0062	n.a.	**n.a.**
27	20.3	n.d.	0.0002	0.0023	0.0047	1323	**2680**
28	20.4	n.d.	0.0003	0.0040	0.0104	1475	**3850**
29	20.6	n.d.	n.d.	0.0045	0.0164	n.a.	**n.a.**
30	20.8	n.d.	0.0002	0.0031	0.0096	1640	**5048**
31	21.0	n.d.	0.0007	0.0009	0.0010	144	150
32	21.5	n.d.	0.0042	0.1545	0.2001	3695	4785
33	22.0	0.0030	0.0028	0.0031	0.0004	110	14
34	22.3	n.d.	n.d.	0.0054	n.d.	n.a.	n.a.
35	22.4	n.d.	n.d.	n.d.	0.0076	n.a.	n.a.
36	23.8	n.d.	0.0003	0.0078	0.0106	2598	3513
37	24.8	n.d.	n.d.	0.0020	n.d.	n.a.	n.a.
38	26.7	0.0271	0.0225	0.0322	0.0100	143	44

39	27.3	0.0654	0.0503	0.0650	0.0747	129	148
40	27.6	0.0078	0.0034	0.0072	0.0083	212	244